

# ***The Moon as a Radiometric Reference for MODIS***

Prepared by

C. Albert McKay  
Research and Data Systems Corp.  
Greenbelt, MD

and

Gerald D. Godden  
Physics Applications Inc.  
Vienna, VA

**September 1996**

Prepared for

The MODIS Characterization Support Team (MCST)  
Code 925  
Goddard Space Flight Center  
Greenbelt, MD

## ABSTRACT

This paper presents average or "representative" Lunar radiance values expected for the MODIS reflective bands when the Moon is viewed by MODIS through the Space View Port and EOS platform maneuvers are not used to enhance Lunar viewing opportunities. The Lunar phase angle for serendipitous views obtained under these conditions is roughly 67.5 degrees. Average Lunar radiance values for the VIS and NIR bands are projected from Lunar irradiance measurements done by Lane and Irvine. Average Lunar radiances in the SWIR bands are obtained from Lunar albedo projections prepared by Hugh H. Kieffer of the U.S. Geological Survey. Lunar radiance values are combined with MODIS required performance parameters to obtain estimates of signal-to-noise ratios, to compare Lunar radiance levels with typical radiance values for Earth scenes, and to compare Lunar radiances with maximum obtainable MODIS readings (full scale) in each of the MODIS reflective bands.

## ***1.0 Introduction***

Consistent long-term Earth data sets are needed to assess the potential effects of man's activities on climate and other Earth systems. The opportunity and challenge facing today's remote sensing scientist is to provide remote sensing data of such long-term accuracy, consistency and reliability that today's data products can serve as an ecological benchmark for future generations. Accuracy of individual data products and consistency among the products of different instruments and programs is achieved by the consistent use of common calibration sources and methods. The basic thought behind the use of the Moon as a radiometric reference is the idea that the reflectance of the Moon is a very stable (estimated change  $10^{-9}$  per year [Kieffer and Wildey 1985]) and the idea that the Moon can serve as a common radiometric reference viewed on-orbit by MODIS and other remote sensing instruments. Conceptually, the Lunar reference could demonstrate that proper and consistent calibration was used among many of the sensors that will be built in the next few decades, and, since the Moon is such an enduring standard, similar verification will be possible even for sensors built in coming centuries by future generations.

One of the Lunar reference strategies proposed for MODIS would use the Moon not as an absolute radiometric standard but as a very precise relative standard useful for detecting changes in sensor responsivity occurring between early on-orbit Lunar views and appropriate later views. This approach is based on the idea that the Lunar radiance at a later viewing will match that of an earlier viewing when the Solar illumination and viewing geometry of the original view recur.

This report primarily discusses Lunar radiometric characteristics as they relate to use of the Moon as a MODIS radiometric reference. Appendix A in this report contains a preliminary discussion of the procedures required to compute the Lunar phase angle and the angular orientation of the Lunar phase pattern. A follow-on report will address Lunar motion and other aspects of Lunar view geometry. Planned future reports will address the relative merits of alternative Lunar strategies and implementation specifics for the techniques chosen for MODIS use.

## 2.0 Average Lunar Spectral Radiance in the MODIS VIS and NIR Bands

Surprisingly few measurements of Lunar radiance or irradiance have been done for the complete Lunar disk. In 1916, H.N. Russell measured an accurate Lunar phase curve (Russell 1916a, 1916b) in the visible spectral region ( $\lambda=550\text{nm}$ ) and in the mid-1930's Rougier measured Lunar irradiance and a phase curve (Rougier 1934, 1937) for mean wavelength  $\lambda=445\text{nm}$ . [The Lunar phase angle is the angle between the observer's view vector and the Solar incident vector as determined at the center of the Moon. The Lunar phase curve expresses the Lunar irradiance at phase angle  $\alpha$  as a fraction of the corresponding Lunar irradiance at full Moon (minimum phase angle for that Lunar phase cycle).] Both of these measurements were done for relatively wide spectral passbands roughly overlapping the human visual response.

Following these early measurements, the next published results for the irradiance of the complete Lunar disk were provided by Lane and Irvine (Lane and Irvine 1973). Their measurements were done using a series of relatively narrow bandpass spectral filters to determine the spectral irradiance of the Moon. Spectral irradiance measurements were done at nine wavelengths ranging from 359 to 1063.5nm and at phase angles ranging from 6 to 120 degrees. Lunar irradiance measurements also were done using three filters with broader bandwidths representing the U (ultraviolet), B (blue), and V (visible) spectral weighting functions used by astronomers for stellar magnitude measurements. Atmospheric extinction for the Moon was computed from corresponding extinction parameters measured for standard reference stars, and ground-measured Lunar irradiances were projected to corresponding top-of-the-atmosphere values. Measured values also were adjusted to unit distance from the Sun and to mean Earth-Moon distance. The Lane and Irvine Lunar irradiance values compare well with the earlier values obtained by Russell and Rougier, and in fact, the spectral behavior measured by Lane and Irvine helps to explain some of the discrepancy observed between the two earlier measurements.

The system of stellar magnitudes in current use is adapted from an earlier system used by the ancient Greeks. By the ancient system, stellar magnitudes of the visible stars ranged from 1 to 6, with magnitude 1 stars being the brightest and magnitude 6 stars being the faintest. In the current system, the relative magnitude of two celestial bodies is determined by the relationship

$$\frac{E_1}{E_2} = 10^{-\left(\frac{m_1 - m_2}{2.5}\right)} \quad (1)$$

where  $m_1$  is the magnitude of the celestial body of irradiance  $E_1$  and  $m_2$  is the corresponding magnitude of the celestial body of irradiance  $E_2$ . The minus sign (magnitude more negative for the brighter celestial body) and the exponent division factor of 2.5 were chosen to maintain consistency with the earlier Greek system.

Absolute stellar magnitudes are obtained from the relative scale defined in Eq. (1) by consistently assigning absolute stellar magnitudes to a series of "standard" reference stars that have been carefully measured and are known to have low intrinsic photometric variability (less than 1 percent). "Standard" stars of known absolute magnitude have been established for all regions of the celestial sphere so that

**Table 1. Measured Lunar Magnitudes at Full Moon as a Function of Wavelength  
(Lane and Irvine, 1973)**

$\lambda(\text{nm})$	359.0	392.6	415.5	457.3	501.2	626.4	729.7	859.5	1063.5
$m$	-12.23	-12.41	-12.45	-12.56	-12.65	-13.11	-13.22	-13.22	-13.35

**Table 2. Phase Curves for the Lunar Disk Expressed in Magnitudes  
(Lane and Irvine, 1973)**

$\lambda(\text{nm})$	359.0	392.6	415.5	457.3	501.2	626.4	729.7	859.5	1063.5
0°	0	0	0	0	0	0	0	0	0
10°	0.29	0.27	0.29	0.28	0.27	0.27	0.26	0.25	0.24
20°	0.58	0.55	0.57	0.56	0.55	0.53	0.52	0.50	0.48
30°	0.86	0.82	0.86	0.83	0.82	0.80	0.77	0.74	0.72
40°	1.15	1.09	1.15	1.11	1.10	1.06	1.03	0.99	0.96
50°	1.41	1.34	1.41	1.37	1.36	1.32	1.28	1.23	1.20
60°	1.66	1.60	1.67	1.62	1.62	1.58	1.54	1.49	1.44
70°	1.93	1.88	1.95	1.90	1.89	1.86	1.82	1.77	1.70
80°	2.23	2.19	2.26	2.20	2.20	2.17	2.13	2.08	1.99
90°	2.59	2.56	2.61	2.55	2.54	2.52	2.48	2.43	2.33
100°	3.01	2.99	3.02	2.95	2.94	2.93	2.87	2.82	2.72
110°	3.51	3.50	3.50	3.42	3.40	3.41	3.32	3.27	3.18
120°	4.11	4.10	4.06	3.98	3.94	3.97	3.83	3.78	3.72

they can be readily referenced independently of the position of the celestial body being measured. Usually a number of standard stars will be referenced during a single magnitude measurement. Corrections for differences in atmospheric extinction may be necessary.

Absolute magnitudes determined using the U, B, and V spectral weighting functions mentioned above are often designated with the letters U, B, and V respectively. A stellar color index can be devised based on magnitude differences observed using different spectral weighting functions. B–V and U–B are the pairs most often used as color indices. A color index of zero has been assigned to a homogeneous group of stars identified as “spectral type AO, luminosity class V”.

The Lunar magnitude results obtained by Lane and Irvine reference the Sun with an absolute Visible magnitude (V) of –26.81 and a color index B–V=0.65. The magnitude scale of each of the narrow spectral bands measured by Lane and Irvine was adjusted so that the corresponding color index for that spectral band (say band X) relative to V for the Sun was zero, i.e. X–V=0 where X is the absolute

magnitude determined for the Sun in Lane and Irvine's spectral band X. Stated differently, Lane and Irvine adjusted the magnitude scale in each of their measured spectral bands so that the magnitude of the Sun in that band (if it could be observed directly with no harm to the instrument) would be  $-26.81$ .

Using these adjusted scales, the magnitudes for the full Moon as extrapolated by Lane and Irvine from their measurements are given in Table 1. Lane and Irvine made measurements for phase angles as small as  $6.6^\circ$  but they avoided measurements at smaller angles to avoid a complicating phenomenon known as "opposition surge" or "opposition effect". Opposition surge is an increase in the brightness of a particulate or other rough surface that occurs as the observer's view direction closely approaches the direction of incident illumination. For celestial bodies, the opposition effect occurs near zero phase angle. The phenomenon was first observed in the rings of Saturn over a century ago (Seeliger 1876, 1895) and the effect has since been observed in the Moon and nearly all the other bodies of the Solar System that present a visible solid surface (Hapke 1986). The opposition effect also has been observed in a wide variety of terrestrial materials.

Seeliger first gave the correct explanation: at zero phase, the shadows produced by the elevated or protruding elements of the surface and the shadows occurring in the crevices or recesses of the surface are not visible to a viewer looking along the direction of the incident illumination, i.e. all elements of the reflecting surface that are visible to the viewer are illuminated by the source and contribute to the return observed by the viewer. A number of mathematical models have been developed to relate oppo-

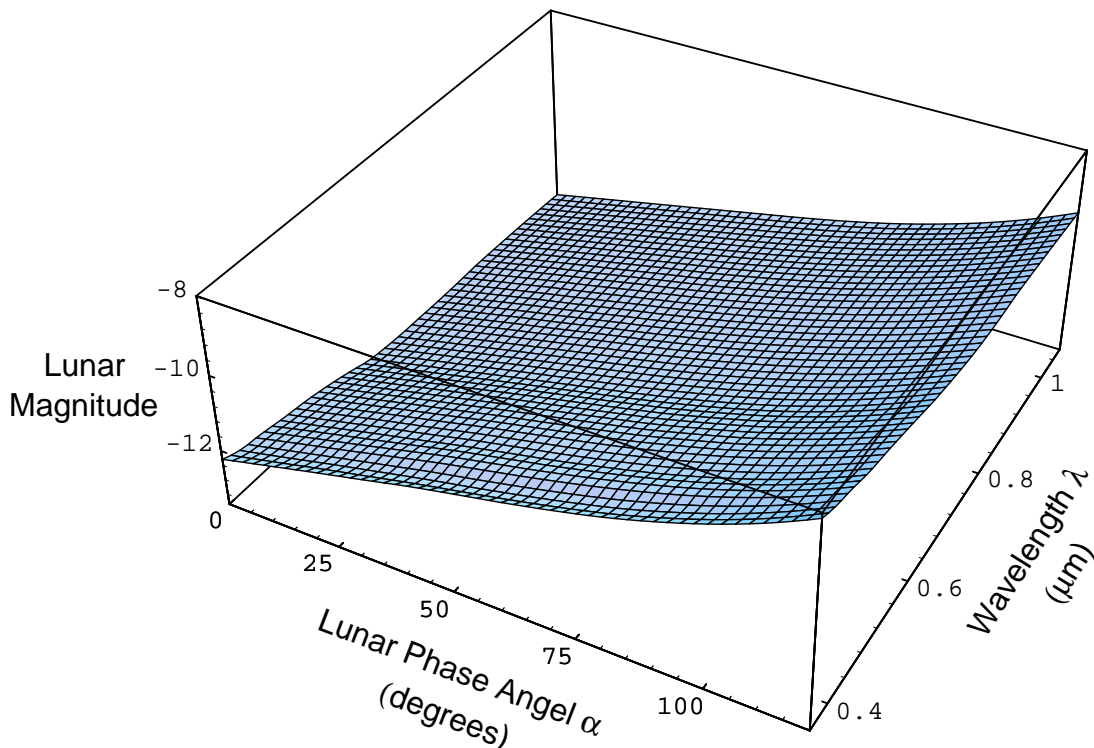


Figure 1. Surface representing the Lunar magnitudes measured by Lane and Irvine. Measurements were done at nine wavelengths ranging from 359 to 1063.5nm and at phase angles ranging from 6 to 120 degrees. Results are expressed relative to the Sun at absolute magnitude  $-26.81$ . A slight reddish tinge is evident in the Lunar reflection.

**Table 3. Center Wavelengths and Bandwidths of the MODIS VIS, NIR, and SWIR Bands**

Band No.	Center Wavelength (nm)	Bandwidth (nm)	Band No.	Center Wavelength (nm)	Bandwidth (nm)
1	645	50	11	531	10
2	858	35	12	551	10
3	469	20	13	667	10
4	555	20	14	678	10
5	1240	20	15	748	10
6	1640	24.6	16	869	15
7	2130	50	17	905	30
8	412	15	18	936	10
9	443	10	19	940	50
10	448	10	26	1375	30

sition brightness to the statistical characteristics of a rough surface (Hapke 1981, 1984, 1986), but the phenomenon is most important near zero phase angle where a slight change in angle can produce appreciable change in brightness. The variation in Lunar brightness near zero phase angle is sometimes called the Hapke function.

The decrease in Lunar irradiance resulting from increased phase angle (the phase law) obtained in the Lane and Irvine measurements is given in Table 2. A surface showing the expected Lunar magnitudes (the full Moon levels given in Table 1 increased by the phase law variations given in Table 2) is shown in Figure 1. Results are presented as a function of Lunar phase angle and wavelength. By Eq.(1) these Lunar magnitudes implicitly relate Lunar irradiance to corresponding Solar irradiance in a narrow passband of interest, and we shall determine average Lunar spectral irradiance in the MODIS bands listed in Table3 by computing the corresponding average Solar spectral irradiance in these same bands.

The average spectral irradiance from the Sun  $\hat{E}_{Sun,i}$  in MODIS spectral band  $i$  is the weighted average of the Solar spectral irradiance  $E_{Sun}(\lambda)$ , where the average is taken using the MODIS transmittance-based system-level response  $\tau_i(\lambda)$  as the spectral weighting function, i.e.

$$\hat{E}_{Sun,i} = \frac{\int_{\tau_i \neq 0} E_{Sun}(\lambda) \tau_i(\lambda) d\lambda}{\int_{\tau_i \neq 0} \tau_i(\lambda) d\lambda} \quad (2)$$

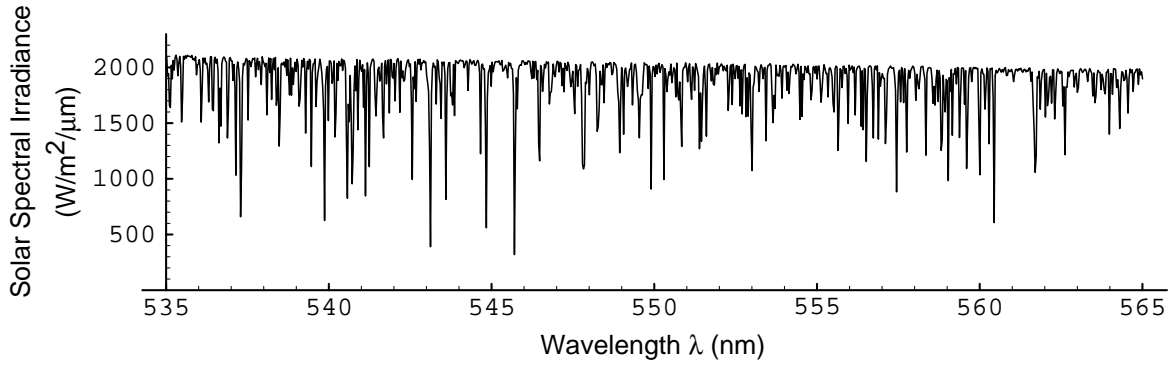


Figure 2. Solar spectral irradiance in the vicinity of Band12 as provided by the Smithsonian Astrophysical Observatory (Kurucz, private communication, 1995). The weighted average Solar spectral irradiance for Band 12 is 1879.5 W/m<sup>2</sup>/μm.

The symbol  $\tau_i \neq 0$  indicates that the integration is to be taken over all measured values of  $\lambda$  for which  $\tau_i(\lambda)$  is not zero. In the computations that follow,  $E_{Sun}(\lambda)$  was obtained from Solar spectra provided by the Smithsonian Astrophysical Observatory (Kurucz, private communication, 1995). Solar spectral irradiance for MODIS Band 12 is plotted in Figure 2; the weighted average Solar spectral irradiance for MODIS Band12 is 1879.5 W/m<sup>2</sup>/μm.  $\tau_i$  was estimated from MODIS Engineering Model and ProtoFlight Model measurements.

The *average* spectral radiance of the Moon can be obtained from the corresponding Lunar irradiance by dividing by the solid angle of the illuminated portion of the Moon. The apparent illuminated area of the Moon (or other spherical body) is computed as a function of phase angle in Appendix B of this report. Converting Lunar area to apparent solid angle, the solid angle  $\Omega(\alpha)$  described by the illuminated portion of the Moon at phase angle  $\alpha$  is related to the solid angle defined by the complete disk,  $\Omega_0$ , by the relationship

$$\Omega(\alpha) = \frac{1 + \cos\alpha}{2} \Omega_0 = \frac{(1 + \cos\alpha)}{2} \frac{\pi R_0^2}{R_{om}^2} \quad (3)$$

where  $R_0$  is the Lunar radius and  $R_{om}$  is the observer-Moon separation..

### 3.0 *Estimated Lunar Spectral Radiance in the MODIS SWIR Bands*

Hugh Kieffer (Kieffer and Wildey 1996) has used the Lane and Irvine observations and laboratory spectral measurements of Apollo 16 Lunar soil samples to prepare an extrapolation of Lunar brightness for the spectral range out to 2.2 μm. This spectral region includes previously unexamined MODIS Bands 5, 6, 7, and 26 (1.240, 1.640, 2.130, and 1.375 μm, respectively). The Kieffer estimates are expressed in terms of “Full-Disk Average Albedo”, a term used by the author to denote an extension of

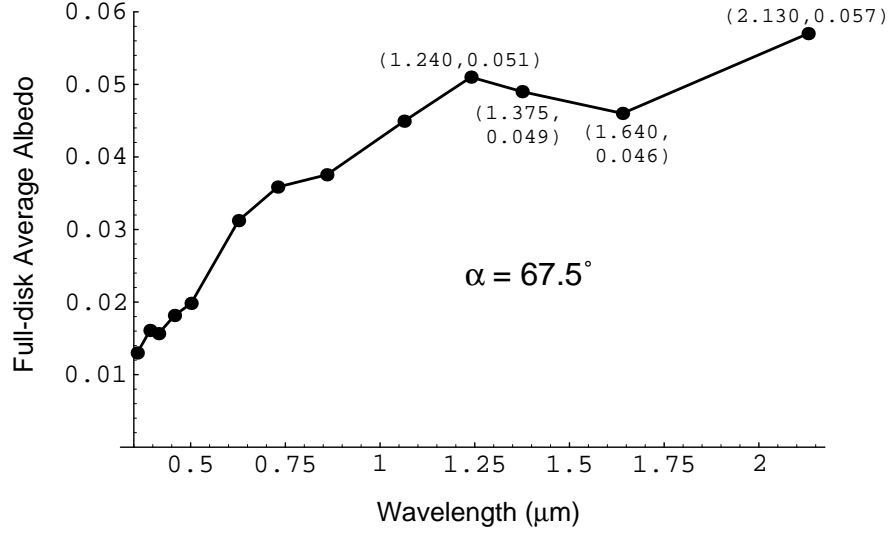


Figure 3. “Full-disk average albedo” values as obtained from Lane and Irvine observations and as extrapolated by Kieffer (Kieffer and Wildey 1996). The extrapolated values are the four points shown with coordinates on the right hand side. These are the projected values for  $\alpha = 67.5^\circ$ . Lunar irradiances corresponding to these albedos are obtained from Eq. (4).

the conventional or geometric albedo for  $\alpha \neq 0$ . (Albedo is normally defined for  $\alpha = 0$ .) The equation relating Full-Disk Average Albedo ( $p$ ) and Lunar irradiance ( $E_m$ ) is (See Appendix C of this report)

$$p = \frac{E_m R_{om}^2}{E_s R_0^2} \quad (4)$$

where  $E_s$  is the Solar irradiance. Figure 3 shows “full disk average albedo” values obtained from the Lane and Irvine observations and as extrapolated to the new spectral domain. Results are given for  $\alpha = 67.5$  degrees. Lunar irradiances corresponding to these albedos are obtained from Eq. (4).

#### 4.0 Radiometric Results for the MODIS VIS, NIR, and SWIR Bands

Applying Eqs. (1) and (4) to the  $\hat{E}_{Sun,i}$  values obtained from Eq. (2) and dividing the resulting Lunar irradiances by the Lunar solid angle described in Eq. (3), we obtain the average Lunar spectral radiances shown in Figure 4 for Lunar phase angle  $\alpha=67.5$  degrees. These values are averages not only in the sense that they are radiances averaged over the illuminated portion of the Lunar disk, but also in the sense that these results assume unit Solar distance and mean separation between the Earth and Moon. Radiances of individual pixels sensed by MODIS will fall both above and below the average values indicated, and high-spatial-resolution spectral radiance measurements would be needed to determine the maximum Lunar radiance that could occur. A phase angle of 67.5 degrees was chosen in



these computations since an analysis of instrument and Lunar geometry has shown that serendipitous views of the Moon through the MODIS Space View Port will occur when the Lunar phase angle is roughly 67.5 degrees. Lunar viewing geometry will be discussed more thoroughly in a future report.

Figure 5 shows the expected average signal-to-noise ratios for MODIS in the Bands indicated. In these computations it was assumed that the sensor noise levels just meet the requirements of the MODIS specification. Figures 6 and 7 show the corresponding expected ratios of average Lunar radiance to the sensor  $L_{typ}$  and the percentage of full scale MODIS reading that the average Lunar radiance represents.

## Bibliography

Hapke, Bruce, "Bidirectional Reflectance Spectroscopy, 1. Theory", *Journal Geophysical Research*, Vol. 86, pp.3039–3054, 1981

Hapke, Bruce, "Bidirectional Reflectance Spectroscopy, 3. Correction for Macroscopic Roughness", *Icarus*, Vol. 59, pp. 41–59, 1984

Hapke, Bruce, "Bidirectional Reflectance Spectroscopy, 4. The Extinction Coefficient and the Opposition Effect", *Icarus*, Vol. 67, pp. 264–280, 1986

Kieffer, Hugh H. and Robert L. Wildey, "Absolute Calibration of Landsat Instruments Using the Moon", *Photogrammetric Engineering and Remote Sensing*, Vol. 51, pp.1391–1393, 1995

Kieffer, Hugh H. and Robert L. Wildey, "Establishing the Moon as a Spectral Radiance Standard", *Journal of Atmospheric and Oceanic Technology*, Vol. 13, No. 2, April 1996

Lane, Adair P. and William M. Irvine, "Monochromatic Phase Curves and Albedos for the Lunar Disk", *The Astronomical Journal*, Vol. 78, No. 3, April 1973

Rougier, G., *L'Astronomie*, Vol. 48, pp.220–233, 1934

Rougier, G., *L'Astronomie*, Vol. 48, pp.281–288, 1934

Rougier, G., *L'Astronomie*, Vol. 51, pg.165, 1937

Russell, H.N., *Astrophysical Journal*, Vol. 43, pg. 103, 1916

Russell, H.N., *Astrophysical Journal*, Vol. 43, pg. 173, 1916

Seeliger, H., Zur Theorie der Beleuchtung der grossen Planeten Insbesondere des Saturn, *Abhandlung der Bayerische Akademie Wissenschaftliche Mathematik-Naturwissenschaft, Klasse II*, Vol. 16, pp.405–516, 1887

Seeliger, H., Theorie der Beleuchtung staubformiger kosmischen Masses Insbesondere des Saturnes, *Abhandlung der Bayerische Akademie Wissenschaftliche Mathematik-Naturwissenschaft, Klasse II*, Vol. 18, pp.1–72, 1895

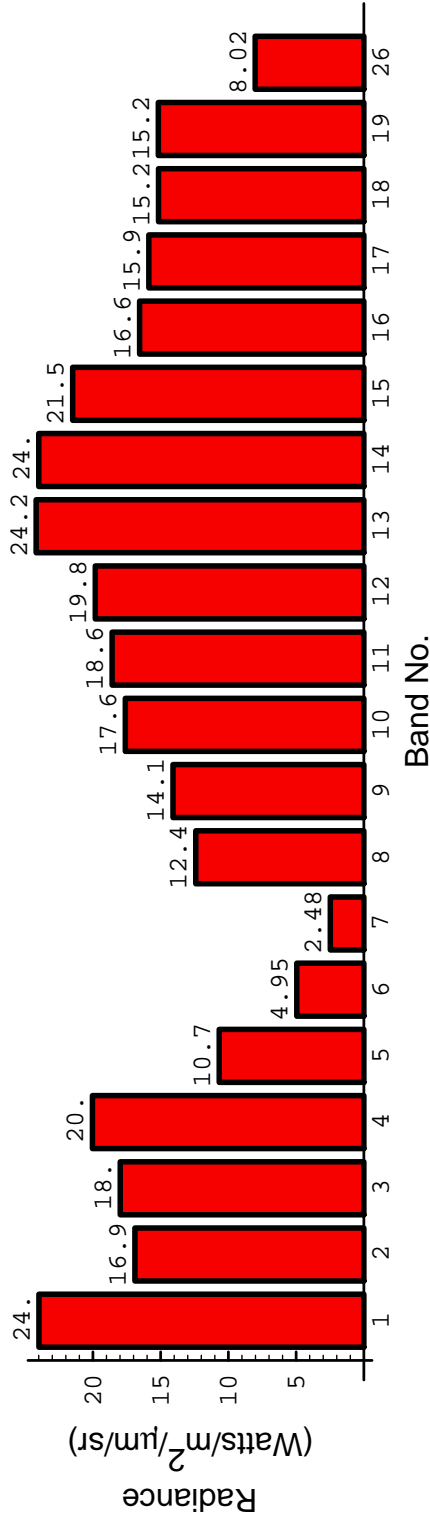


Figure 4. Average or "representative" Lunar radiance on the illuminated portion of the Lunar disk at a phase angle of 67.5 degrees. Individual MODIS pixels on the illuminated portion of the disk will fall both above and below the given values. High-spatial-resolution spectral radiance measurements would be needed to determine the maximum Lunar radiance that could occur. Serendipitous views of the Moon will occur at the MODIS Space View Port when the Lunar phase angle is approximately 67.5 degrees

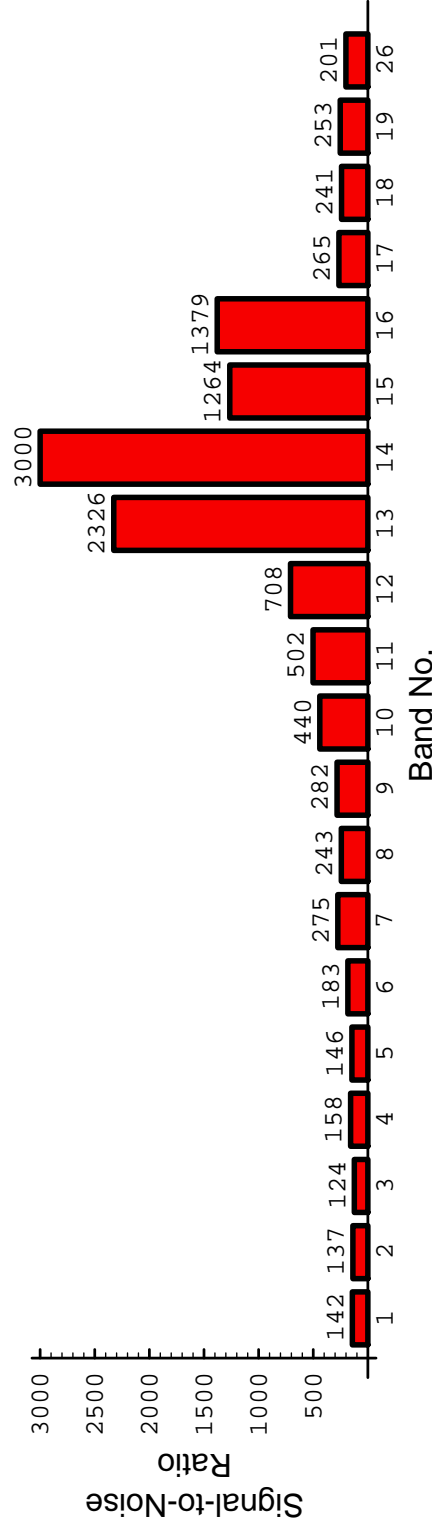


Figure 5. Average or "representative" MODIS signal-to-noise ratios corresponding to the Lunar radiances given in Figure 2. The noise levels in these computations were taken from the MODIS specification.

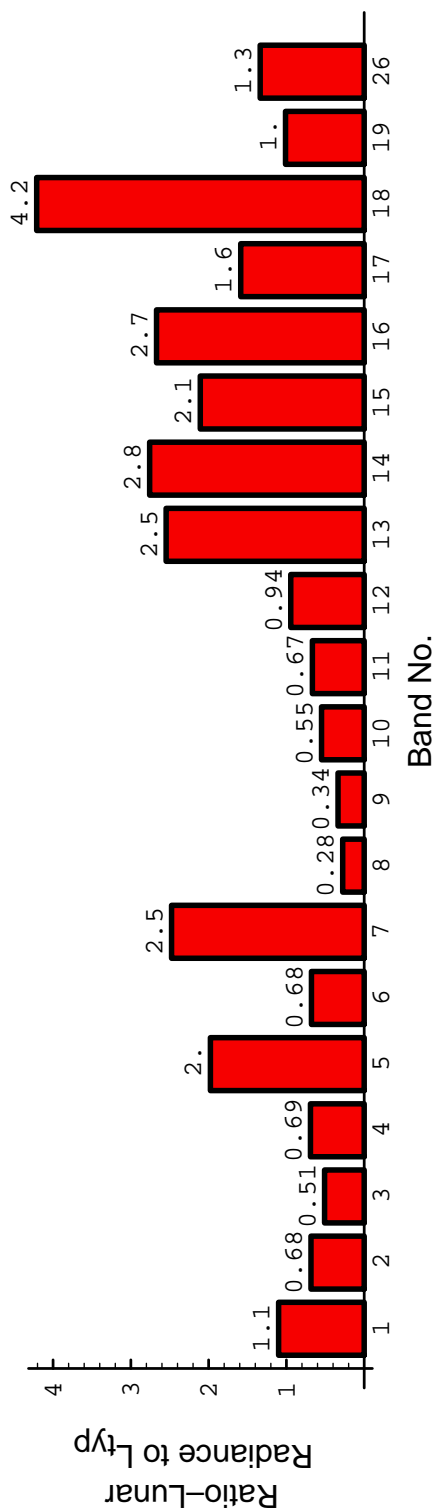


Figure 6. Average or “representative” ratios of Lunar radiance to  $L_{typ}$  for the MODIS bands indicated. Actual values will fall both above and below the values given.

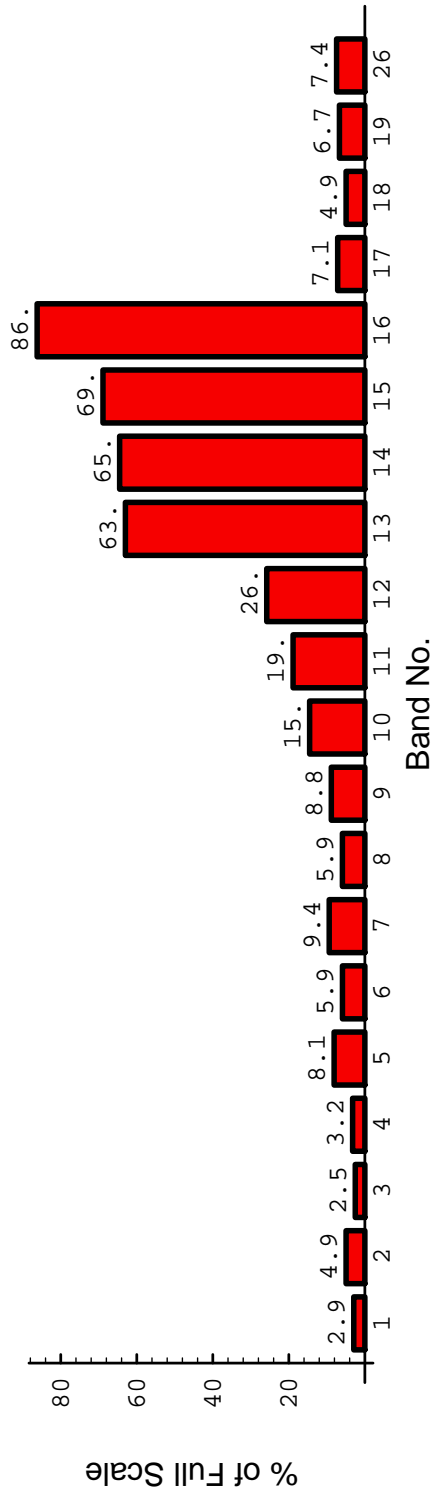


Figure 7. Average or “representative” percent of full scale corresponding to the Lunar radiances given in Figure 4.

## Appendix A

### Computation of Lunar Geometric Parameters

Consider a three dimensional coordinate system  $xyz$  in which the position of the Sun is given by  $\mathbf{r}_s$ , the position of the Moon is given by  $\mathbf{r}_m$  and the position of a Lunar observer is given by  $\mathbf{r}_o$ . Then the Sun to Moon distance is given by

$$R_{sm} = |\mathbf{R}_{sm}| = \sqrt{(\mathbf{r}_m - \mathbf{r}_s) \cdot (\mathbf{r}_m - \mathbf{r}_s)}$$

and Solar radiation strikes the Moon from the direction given by unit vector

$$\hat{\mathbf{n}}_{sm} = \frac{\mathbf{r}_m - \mathbf{r}_s}{R_{sm}}.$$

Likewise the observer to Moon distance is

$$R_{om} = |\mathbf{R}_{om}| = \sqrt{(\mathbf{r}_m - \mathbf{r}_o) \cdot (\mathbf{r}_m - \mathbf{r}_o)}$$

and the observer view direction is

$$\hat{\mathbf{n}}_{om} = \frac{\mathbf{r}_m - \mathbf{r}_o}{R_{om}}.$$

The Lunar phase angle  $\alpha$  is defined as the angle between the center of the Sun and the observer as determined at the center of the Moon. The magnitude of  $\alpha$  can be computed from the relation

$$\cos \alpha = \hat{\mathbf{n}}_{sm} \cdot \hat{\mathbf{n}}_{om}.$$

Usually, phase angles for the waxing Moon (increasing in brightness) are considered negative and phase angles for the waning Moon (decreasing in brightness) are considered positive. If Lunar cycles are measured between successive new moons (synodical month), then by this convention negative phase angles precede positive ones.

If the orientation of the Lunar phase pattern ( $\phi$ ) is designated by the direction to the Sun relative to the Lunar center in the sensor image, orientation can be defined by the projections of the Moon to Sun unit vector ( $-\hat{\mathbf{n}}_{sm}$ ) on two mutually orthogonal axes, say unit vectors in the direction of increasing scan ( $\hat{\mathbf{e}}_{scan}$ ) and increasing track ( $\hat{\mathbf{e}}_{track}$ ) where  $\hat{\mathbf{e}}_{scan}$  and  $\hat{\mathbf{e}}_{track}$  are referenced to the sensor image. If computations are done in instrument based coordinates,  $\hat{\mathbf{e}}_{scan}$  and  $\hat{\mathbf{e}}_{track}$  must be transformed to instrument coordinates before the components are computed. Designating the transformed components of  $\hat{\mathbf{e}}_{scan}$  and  $\hat{\mathbf{e}}_{track}$  by  $\tilde{\mathbf{e}}_{scan}$  and  $\tilde{\mathbf{e}}_{track}$ , respectively, the scan and track components of  $-\hat{\mathbf{n}}_{sm}$  can be written

$$\begin{aligned} n_{scan} &= -\hat{\mathbf{n}}_{sm} \cdot \tilde{\mathbf{e}}_{scan} \\ n_{track} &= -\hat{\mathbf{n}}_{sm} \cdot \tilde{\mathbf{e}}_{track} \end{aligned}$$

and we can then write

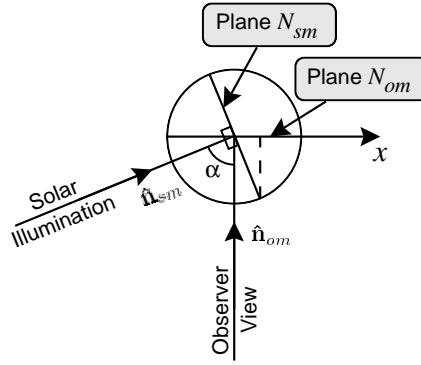
$$\phi = \arctan2(n_{scan}, n_{track})$$

where  $\arctan2(x, y)$  designates the arctangent function of type 2.  $\arctan2(x, y)$  assigns the proper quadrant to arctangent results based on the signs of the  $x$  and  $y$  arguments.

## Appendix B

### Illuminated Area of a Spherical Celestial Body

Consider a spherical celestial body of radius  $R_0$  illuminated by the Sun from a direction given by unit vector  $\hat{\mathbf{n}}_{sm}$ . Let  $N_{sm}$  be the plane perpendicular to  $\hat{\mathbf{n}}_{sm}$  that passes through the center of the sphere. Note that  $N_{sm}$  divides the sphere into illuminated and dark hemispheres. Similarly, let  $\hat{\mathbf{n}}_{om}$  be the unit vector denoting an observer's view direction and let  $N_{om}$  be the plane perpendicular to  $\hat{\mathbf{n}}_{om}$  also passing through the center of the sphere. Note that, from the observer's perspective,  $N_{om}$  divides the sphere into visible and invisible hemispheres. The angle between planes  $N_{om}$  and  $N_{sm}$  is the phase angle  $\alpha$ . Attach  $xy$ -coordinates to the celestial body with the  $y$ -axis along the line of intersection of the planes and the  $x$ -axis in the plane  $N_{om}$ .



Consider the boundaries of the illuminated area visible to the observer (intersection of the illuminated and visible hemispheres, as discussed above). On the illuminated side (left in the figure), the  $x$ -coordinate of the boundary is

$$x = -\sqrt{R_0^2 - y^2}$$

and on the other side

$$x = \sqrt{R_0^2 - y^2} \cos \alpha$$

since the angle between planes  $N_{om}$  and  $N_{sm}$  is  $\alpha$ . Then integrating in the vertical dimension, the illuminated area  $\mathcal{A}$  is given by

$$\mathcal{A} = \int_{-R_0}^{R_0} \sqrt{R_0^2 - y^2} dy + \int_{-R_0}^{R_0} \sqrt{R_0^2 - y^2} \cos \alpha dy$$

or collecting terms

$$\mathcal{A} = (1 + \cos \alpha) \int_{-R_0}^{R_0} \sqrt{R_0^2 - y^2} dy.$$

Substituting  $y = R_0 \sin \vartheta$ ,  $dy = R_0 \cos \vartheta d\vartheta$ , and

$$\mathcal{A} = (1 + \cos \alpha) R_0^2 \int_{-\pi/2}^{\pi/2} \cos^2 \vartheta d\vartheta.$$

Again substituting

$$\cos^2 \vartheta = \frac{1 + \cos 2\vartheta}{2}$$

and carrying out the indicated integration

$$\mathcal{A} = (1 + \cos \alpha) R_0^2 \frac{\pi}{2}$$

or

$$\mathcal{A} = \left( \frac{1 + \cos \alpha}{2} \right) \pi R_0^2$$

i.e. the apparent illuminated area of a sphere of radius  $R_0$  is the area of the associated disk of the same radius ( $\pi R_0^2$ ) times a phase factor

$$\left( \frac{1 + \cos \alpha}{2} \right)$$

that describes the decrease in illuminated area as the phase angle increases or decreases from  $\alpha = 0$ .

## Appendix C

### Albedo and Lunar Irradiance

The conventional or geometric albedo ( $p$ ) of a celestial object is defined as the ratio of the irradiance of the object at phase angle  $\alpha = 0$  to the corresponding irradiance of a perfectly diffusing disk (Lambertian and non-absorbing) at the same position and with the same apparent size as the celestial object. If  $E_{m0}$  is the Lunar irradiance at  $\alpha = 0$  and  $E_{ref}$  is the irradiance of the idealized reference disk

$$p = \frac{E_{m0}}{E_{ref}}. \quad (1)$$

We shall compute  $E_{ref}$ . If the irradiance of the Sun at the Lunar center is  $E_s$ , the radiance at the surface of the reference disk is

$$L_{ref} = \frac{d^2\Phi_{ref}}{d\omega ds} = \frac{1}{\pi} E_s \quad (2)$$

since the reference surface is Lambertian. All quantities are relative to the surface of the reference disk. Since  $L_{ref}$  is constant across the entire reference surface, the intensity of the surface may be obtained simply by multiplying  $L_{ref}$  by the area of the reference surface:

$$I_{ref} = \frac{d\Phi_{ref}}{d\omega} = \pi R_0^2 L_{ref} \quad (3)$$

where  $R_0$  is the radius of the celestial object. Likewise, the differential flux falling on an observing apparatus of capture area  $dA$  separated by a distance  $R_{om}$  from the reference surface is

$$d\Phi_{ref} = I_{ref} d\omega = I_{ref} \frac{dA}{R_{om}^2}. \quad (4)$$

Combining (2-4) and solving for  $E_{ref}$

$$E_{ref} = \frac{d\Phi_{ref}}{dA} = E_s \frac{R_0^2}{R_{om}^2}. \quad (5)$$

and finally, returning to (1) we obtain

$$p = \frac{E_{m0}}{E_s} \frac{R_{om}^2}{R_0^2}. \quad (6)$$

Note that, properly speaking, the geometric albedo  $p$  is defined only for  $\alpha = 0$ .